catalysts

MDPI

Article

The Role of Fe_2O_3 Species in Depressing the Formation of N_2O in the Selective Reduction of NO by NH_3 over V_2O_5/TiO_2-Based Catalysts

Moon Hyeon Kim * and Ki Hyuck Yang

Department of Environmental Engineering, Daegu University 201 Daegudae-ro, Jillyang, Gyeongsan 38453, Korea; wiws3@naver.com

* Correspondence: moonkim@daegu.ac.kr; Tel.: +82-53-850-6693; Fax: +82-53-850-6699

Received: 28 February 2018; Accepted: 27 March 2018; Published: 30 March 2018

Abstract: Promotion of 2.73% Fe_2O_3 in an in-house-made V_2O_5-WO_3/TiO_2 (VWT) and a commercial V_2O_5-WO_3/TiO_2 (c-VWT) has been investigated as a cost effective approach to the suppression of N_2O formation in the selective catalytic reduction of NO by NH_3 (NH_3-SCR). The promoted VWT and c-VWT catalysts all gave a significantly decreased N_2O production at temperatures >400 °C compared to the unpromoted samples. However, such a promotion led to the loss in high temperature NO conversion, mainly due to the oxidation of NH_3 to N-containing gases, particularly NO. Characterization of the unpromoted and promoted catalysts using X-ray diffraction (XRD), NH_3 adsorption-desorption, and Raman spectroscopy techniques could explain the reason why the promotion showed much lower N_2O formation levels at high temperatures. The addition of Fe_2O_3 to c-VWT resulted in redispersion of the V_2O_5 species, although this was not visible for 2.73% Fe_2O_3/VWT. The iron oxides exist as a highly-dispersed noncrystalline α-Fe_2O_3 in the promoted catalysts. These Raman spectra had a new Raman signal that could be tentatively assigned to Fe_2O_3-induced tetrahedrally coordinated polymeric vanadates and/or surface V-O-Fe species with significant electronic interactions between the both metal oxides. Calculations of the monolayer coverage of each metal oxide and the surface total coverage are reasonably consistent with Raman measurements. The proposed vanadia-based surface polymeric entities may play a key role for the substantial reduction of N_2O formed at high temperatures by NH_3 species adsorbed strongly on the promoted catalysts. This reaction is a main pathway to greatly suppress the extent of N_2O formation in NH_3-SCR reaction over the promoted catalysts.

Keywords: NH_3-SCR reaction; V_2O_5-WO_3/TiO_2 catalyst; N_2O formation; Fe_2O_3 promotion; NH_3 oxidation; Raman spectra

1. Introduction

Commercially-available, anatase-type TiO_2-supported V_2O_5 catalysts with either WO_3 or MoO_3 as a structure stabilizer of the support and a surface acidity enhancer are typical for selective catalytic reduction (SCR) of NO_x from relatively large scale stationary and mobile sources in the presence of N-containing reductants, such as gaseous NH_3 and aqueous urea [1,2]. They are usually formulated to 0.1–3% V_2O_5 and 7–10% WO_3 or 6–10% MoO_3 [3–8], depending on industrial application target, and V_2O_5-WO_3/TiO_2 systems are prevailed for such deNO_x processes. The overall NH_3-SCR reaction with V_2O_5/TiO_2-based catalysts could be adequately described by [5–7]:

$$4NO + 4NH_3 + O_2 \rightarrow 4N_2 + 6H_2O, \quad (1)$$

$$NO + NO_2 + 2NH_3 \rightarrow 2N_2 + 3H_2O. \quad (2)$$

The standard Reaction (1) takes place in the presence of excess oxygen, while Reaction (2) has been known as the fast SCR pathway in an equimolar mixture of NO and NO_2 and is known to be much faster than the Reaction (1) at low temperatures [6,9,10].

In addition to the main SCR reactions over V_2O_5-WO_3 (or MoO_3)/TiO_2 catalysts, many side reactions can occur, and among them, one is the production of N_2O that is a greenhouse gas with a global warming potential of 310 at a 100-year time horizon, and the extent of its emissions can greatly depend on the loading and crystallinity of V_2O_5, the secondary component, reaction temperature, concentrations of H_2O and O_2, and so forth [3,6,11–15]. Such a formation of N_2O in the NH_3-SCR reaction is proposed by the following major routes [6,12–15]:

$$4NO + 4NH_3 + 3O_2 \rightarrow 4N_2O + 6H_2O \quad (3)$$

$$2NH_3 + 2O_2 \rightarrow N_2O + 3H_2O. \quad (4)$$

These reactions predominantly occur at high temperatures when V_2O_5-WO_3/TiO_2 catalysts are employed for deNO_x SCR reaction and are associated with a decrease in high-temperature NO conversion and N_2 selectivity [12–15].

An attempt to minimize the formation of N_2O in NH_3-SCR processes has been reported: a direct coating of Fe-ZSM-5 onto a commercial V_2O_5-WO_3/TiO_2 catalyst [16], a sequential configuration of V_2O_5-WO_3/TiO_2 and Fe-ZSM-5 [17], and a modification of TiO_2 using Fe_2O_3 before V_2O_5 and WO_3 loadings [18,19]. These studies were started from the fact that Fe-exchanged zeolites, representatively Fe-ZSM-5, are a commercially proven catalyst not only for the NH_3-SCR reaction but also for direct N_2O decomposition; thereby, the decomposition of N_2O produced in the SCR reaction into N_2 on Fe ions and/or its reduction by residual NH_3 species [20–23] is expected, and from that a nanosized iron oxide, γ-Fe_2O_3 (maghemite), is active for the NH_3-SCR reaction, although N_2O production levels were not addressed for this system [24]. The Fe-ZSM-5-coated V_2O_5-WO_3/TiO_2 catalysts could greatly depress the formation of N_2O in NH_3-SCR reaction, depending on the coating content [16], unlike the series configuration systems [17]. Samples of coprecipitated, Fe_2O_3-TiO_2-supported 1% V_2O_5, and 1% V_2O_5-10% WO_3/TiO_2, had similar NO conversions at 150–400 °C but at higher temperatures, lower ones, depending on the temperature, were indicated for the former sample [18]. This showed a better N_2 selectivity at high temperatures $\geq$400 °C [18]; however, this observation may be apparent because of the difference in NO conversion at the temperature region between the catalysts. All 1% V_2O_5-10% WO_3 catalysts dispersed on 1–5% Fe_2O_3/TiO_2 gave an improvement to N_2 selectivity at temperatures >450 °C, compared to the bare TiO_2-based catalyst; in addition to that, they showed higher NO conversion below 350 °C but comparable NO conversion at higher temperatures [19].

Unsupported and supported Fe_2O_3 are still suspicious of the tolerance to SO_2 existing in flue gases, depending strongly on their preparation techniques [19,24–26], but this point can be avoided for no sulfur applications, such as natural gas-fired plants. The earlier approaches to the reduction in N_2O emissions from NH_3-SCR reaction could advise us of an efficient way of promoting V_2O_5-WO_3/TiO_2 catalysts using Fe_2O_3. Such a utilization of Fe_2O_3 is cost effective, compared to Fe-zeolites whose preparation requires more complicated, expensive processes. Therefore, we have studied a promotional effect of Fe_2O_3 in samples of laboratory-made V_2O_5-WO_3/TiO_2 and commercial V_2O_5-WO_3/TiO_2 on the suppression of N_2O production in NH_3-SCR reaction. The Fe_2O_3 as a promoter was added to the V_2O_5/TiO_2-based catalysts using the well-known impregnation technique, and this is much simpler than the utilization of a coprecipitated Fe_2O_3-TiO_2 and a Fe_2O_3-coated TiO_2 to support V_2O_5 and WO_3 reported in the literature.

2. Results and Discussion

2.1. Physicochemical Properties of Fe_2O_3-Promoted V_2O_5-WO_3/TiO_2 Catalysts

X-ray diffraction (XRD) patterns for VWT, 2.73% Fe_2O_3/VWT, c-VWT, and 2.73% Fe_2O_3/c-VWT at a 2θ value of 10–80° are shown in Figure 1. All the catalysts gave a predominant peak at 2θ = 25.31° with much smaller diffractions at higher 2θ values, as displayed in Figure 1a–d, and all these peaks were the same as those existing in the pattern for anatase TiO_2 shown in Figure 1e. No diffraction due to the crystalline WO_3 was shown for all the samples, indicating that WO_3 existing in them is amorphous WO_x species [27]. There was also no presence of crystalline V_2O_5 phases, except for c-VWT, in which a weak reflection near 2θ = 21.64° appeared when the diffraction was magnified, as indicated in Figure 1c, which is assigned to the crystallographic (101) plane of a polycrystalline α-V_2O_5 (JCPDS card # 41-1426) by comparing it with the pure reference V_2O_5 with an orthorhombic structure as provided in Figure 1f [27,28]. However, the XRD peak disappeared in 2.73% Fe_2O_3/c-VWT, as shown in the magnified pattern in Figure 1d. It should be mentioned that all of the other catalysts gave no peak at the 2θ value, even in similar magnified spectra (not shown here).

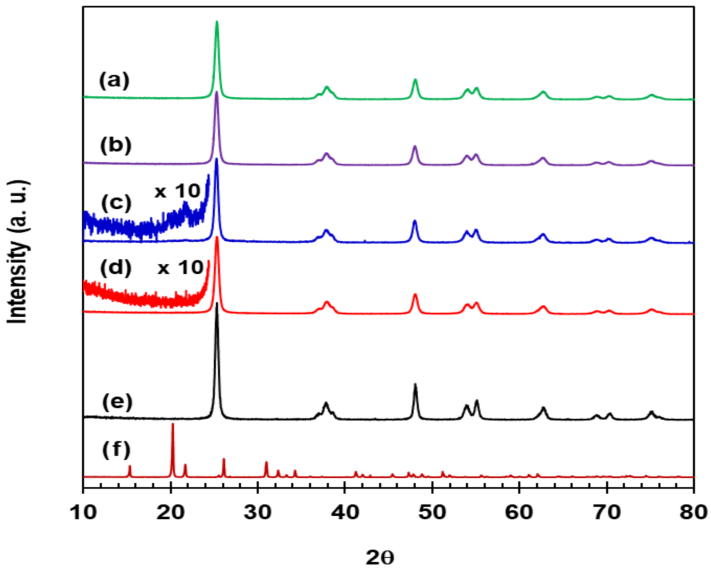

Figure 1. XRD patterns for: (**a**) VWT; (**b**) 2.73% Fe_2O_3/VWT; (**c**) c-VWT; (**d**) 2.73% Fe_2O_3/c-VWT; (**e**) pure anatase TiO_2; and (**f**) α-phase orthorhombic V_2O_5.

Comparing hematite (α-Fe_2O_3), maghemite (γ-Fe_2O_3), magnetite (Fe_3O_4), goethite (α-FeOOH), akaganeite (β-FeOOH), lepidocrocite (γ-FeOOH), and feroxyhyte (δ-FeOOH) in the corresponding JCPDS card #s 33-0664, 39-1346, 02-1035, 29-0713, 34-1266, 08-98, and 29-712, neither of them were indicated in XRD patterns for 2.73% Fe_2O_3-promoted catalysts, as disclosed in Figure 1b,d. Even a sample of 8% Fe_2O_3/VWT after calcination at 500 °C gave no crystalline peaks due to the iron compounds (not shown here). Magnetite nanoparticles are easily transformed to γ-Fe_2O_3 and α-Fe_2O_3 when, respectively, calcined at 300 and 500 °C in air [29], and all the FeOOH phases can be altered to α-Fe_2O_3 even at relatively lower thermal energy [30]. Our XRD measurements, and the thermal stability of the iron oxides and oxyhydroxides, reasonably indicate that FeO_x species existing in the promoted catalysts are in the form of α-Fe_2O_3 as a highly-dispersed noncrystalline particle, and that the Fe_2O_3 could significantly interact with V_2O_5 in c-VWT, thereby resulting in redispersion of the V_2O_5.

2.2. Textural Features of Fe_2O_3-Promoted V_2O_5-WO_3/TiO_2 Catalysts

N_2 sorption isotherm of 2.73% Fe_2O_3/VWT was similar to that measured for VWT and WT, as provided in Figure 2a–c. This case was the same for c-VWT and 2.73% Fe_2O_3/c-VWT (Figure 2d,e).

All the isotherms showed a typical character of mesoporous materials because of the desorption hysteresis at P/P_o = 0.53–0.67 [31], depending on the sample.

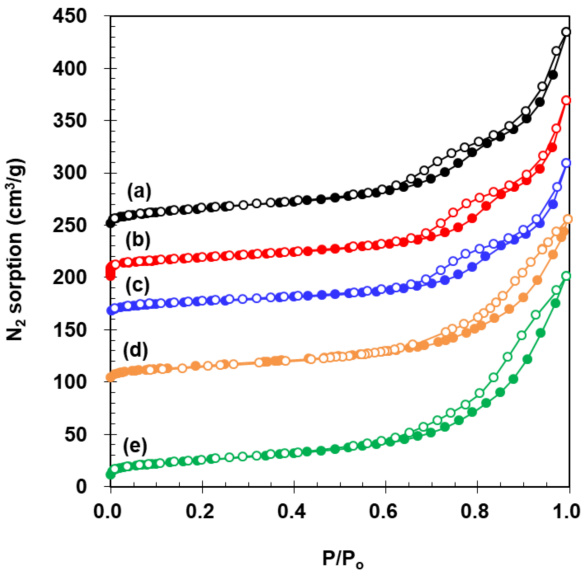

Figure 2. N_2 sorption isotherms on: (**a**) WT; (**b**) VWT; (**c**) 2.73% Fe_2O_3/VWT; (**d**) c-VWT; and (**e**) 2.73% Fe_2O_3/c-VWT.

Values for the specific BET surface area (S_{BET}), the mesopore size (d_m), and the total pore volume (V_t) are listed in Table 1. The S_{BET} value of WT decreased upon 1.6% V_2O_5 loading, which is due to some blockage of relatively small pores by the vanadia, but a further decrease after 2.73% Fe_2O_3 addition to the VWT was insignificant. These are consistent with changes in values for d_m and V_t. On the other hand, the promotion of c-VWT using 2.73% Fe_2O_3 led to an increased S_{BET} compared to the bare sample, and yielded somewhat smaller d_m and larger V_t values (Table 1). This might be caused by rearrangement of mechanical additives existing in c-VWT, such as glass fibers, during the sample preparation using an aqueous solution of the iron precursor [6,32,33].

Table 1. Chemical compositions and textural properties of V_2O_5/TiO_2-based catalysts.

Catalyst	Amount (%)		S_{BET} (m^2/g)	d_m (Å) [a]	V_t (cm^3/g) [b]
	V_2O_5	WO_3			
WT	-	10	91	127	0.30
VWT	1.6	10	67	142	0.26
2.73% Fe_2O_3/VWT	1.6	10	60	139	0.23
c-VWT	1.44	9.42	70	144	0.27
2.73% Fe_2O_3/c-VWT	1.44	9.42	89	126	0.31

Note. "-": not applicable or measured; S_{BET}: specific BET surface area; d_m: mesopore size; V_t: total pore volume. [a] Using the Barrett-Joyner-Halenda (BJH) mesopore model. [b] Calculated using N_2 sorption amounts at $P/P_o \approx 0.994$.

2.3. *Effect of Fe_2O_3 Species on NH_3-SCR Reaction and N_2O Formation*

Conversions of NO and NH_3 in $deNO_x$ reaction with VWT, 2.73% Fe_2O_3/VWT, c-VWT, and 2.73% Fe_2O_3/c-VWT and N_2O production are shown in Figures 3 and 4, respectively. The VWT-only exhibited 100% NO conversion at 300–400 °C, while at higher temperatures, it decreased depending on the temperature, as provided in Figure 3a. This shape of activity loss is a common feature of NH_3-SCR reaction over V_2O_5/TiO_2-based catalysts due to some side reactions giving N_2O, N_2, and NO [1,13,34]. The commercial unpromoted catalyst, i.e., c-VWT, basically showed a similar

temperature vs. $deNO_x$ activity. These behaviors are consistent with those reported for 1.7–3.5% V_2O_5 dispersed on a commercial 10% WO_3/TiO_2 [1], 1.5% V_2O_5-10% WO_3/TiO_2 [35], and 1–5% V_2O_5 on four different commercial WO_3/TiO_2 supports with a WO_3 content of 4.7–6.8% [36]. After addition of 2.73% Fe_2O_3 to VWT and c-VWT, these all gave a significant decrease in NO conversion above 400 °C. As an example, the 2.73% Fe_2O_3/VWT had a NO conversion of 60% at 480 °C, which is lower, by 20%, than that indicated over the unpromoted catalyst. In case the 2.73% Fe_2O_3/c-VWT was used, the extent of such a decrease was much smaller.

Figure 3b shows NH_3 conversions over the unpromoted and promoted catalysts. Each value for NH_3 conversion below 400 °C could be comparable to that indicated for NO (Figure 3a), which is consistent with the overall reaction described by Equations (1) and (2). However, at higher temperatures the value was 100% regardless of the catalyst employed, and there is a difference in conversion between NH_3 and NO. This discrepancy depended not only on the catalyst employed but also on the presence of the iron oxide. The extent of the difference was smaller over the laboratory-made VWT than over the c-VWT, but this trend was reversed when 2.73% Fe_2O_3 was promoted to VWT and c-VWT (Figure 3a,b). Consequently, it is definitely represented that besides the general SCR mechanism, NH_3 would be consumed via undesired pathways at high temperatures >400 °C.

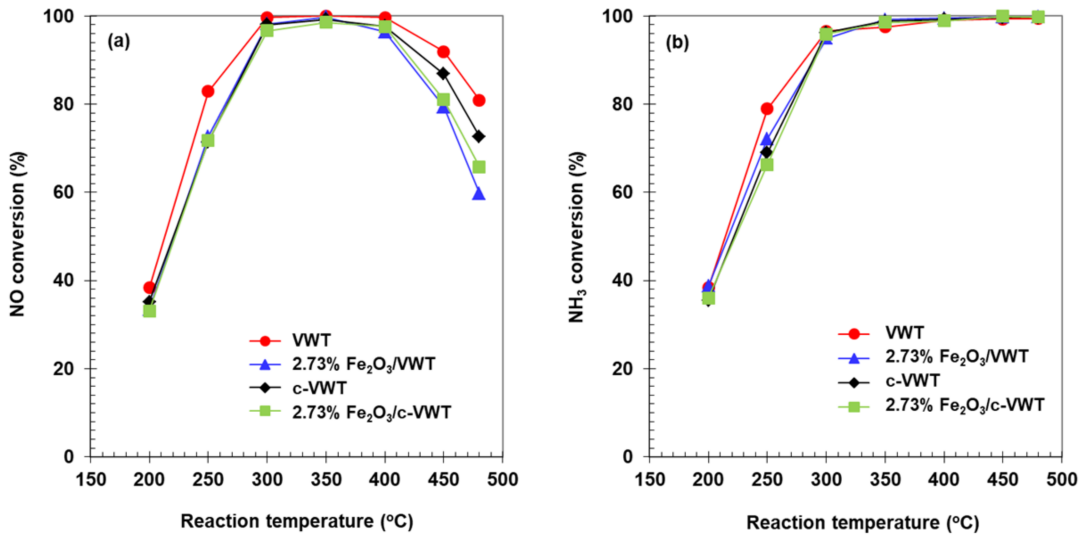

Figure 3. Conversions of (**a**) NO and (**b**) NH_3 in the reduction of NO by NH_3 over unpromoted and Fe_2O_3-promoted V_2O_5/TiO_2-based catalysts.

N_2O could be produced over V_2O_5-WO_3 (or MoO_3)/TiO_2 catalysts widely used for stationary and mobile applications and it can approach about 750 ppm depending strongly on the catalyst formulation and reaction conditions [8,13,37]. Whether or not the formation of N_2O in NH_3-SCR reaction with Fe_2O_3-promoted V_2O_5-WO_3/TiO_2 catalysts can be significantly depressed is of particular interest. Results are provided in Figure 4. A comparison between VWT and 2.73% Fe_2O_3/VWT indicated that the Fe_2O_3 promotion can greatly suppress N_2O production. That is, the VWT catalyst had, respectively, ca. 60 and 110 ppm N_2O at 450 and 480 °C, but the respective values decreased to about 25 and 45 ppm over the promoted VWT sample, corresponding to a reduction by 60% regardless of the temperature. This catalyst lost a NO conversion by 12–20% at 450–480 °C, compared to that observed for the VWT-only (Figure 3a). Although the indicated difference in NO conversion between c-VWT and 2.73% Fe_2O_3/c-VWT at temperatures >400 °C was less than 10% (Figure 3a), a depression effect on N_2O formation was similar to that of the promoted VWT catalyst (Figure 4). It represents that the Fe_2O_3 species in the VWT and c-VWT can be responsible for significant reduction in N_2O emissions from NH_3-SCR reaction at high temperatures.

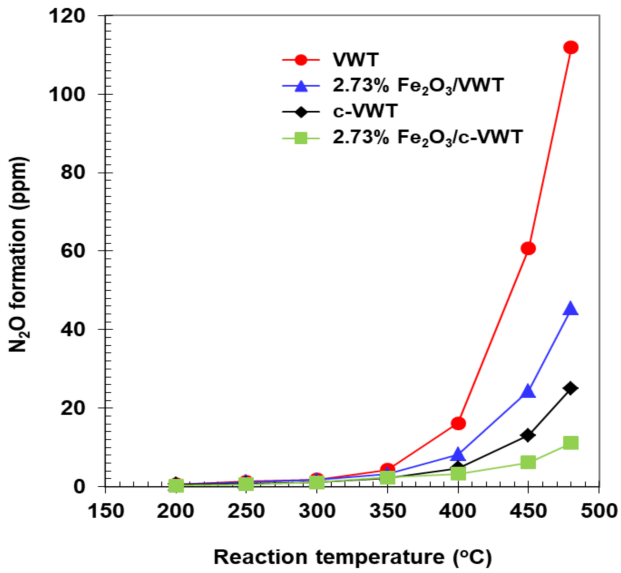

Figure 4. Formation of N_2O in the reduction of NO by NH_3 over unpromoted and Fe_2O_3-promoted V_2O_5/TiO_2-based catalysts.

The small changes in the textural properties of the Fe_2O_3-promoted catalysts (Table 1) might not contribute to the observed decrease in both NO removal and N_2O formation above 400 °C, because these reactions are predominantly determined by chemical compositions rather than textural features [8,38]. A commercial V_2O_5-WO_3/TiO_2 catalyst after prolonged usage at industrial deNO$_x$ plants could yield a large amount of N_2O via Equation (3) at high temperatures [6]. However, low N_2O production over the Fe_2O_3-promoted catalysts may not be due to significant inactivation of Equation (3), since in this circumstance, all NO and NH_3 conversions shall decrease by Equation (1). If the observed decrease in the NO conversion were because of Equation (4), the extent of the N_2O formed should increase. Based on the discussion, and the measured data for NO and NH_3 conversions, it is proposed that the oxidation of NH_3 into NO over the promoted catalysts at high temperatures,

$$4NH_3 + 5O_2 \rightarrow 4NO + 6H_2O, \quad (5)$$

could occur. Thus, the NO gives rise to the decrease in deNO$_x$, activity while NH_3 conversion is still high. Such a NO generation even at 300 °C can take place over Fe_2O_3-containing mixed metal oxides, such as Fe_2O_3-TiO_2, which has been also highly active for NH_3-SCR reaction [39]. A 3% V_2O_5-9% WO_3/TiO_2 catalyst shows the formation of NO in NH_3 oxidation at temperatures >425 °C, depending on concentrations of O_2 in a feed gas stream [14]. Consequently, the addition of Fe_2O_3 to V_2O_5/TiO_2-based catalysts depresses the formation of N_2 in NH_3-SCR reaction at high temperatures, but unfortunately this approach can accompany the undesired pathway.

Another interest to us is whether or not different N_2O production levels of unpromoted and Fe_2O_3-promoted catalysts could result in a difference in absolute NO conversion between them. VWT had a NO conversion near 80% at 480 °C, and a similar value could be exhibited over 2.73% Fe_2O_3/VWT at 450 °C (Figure 3a). Therefore, both samples should give 50 ppm N_2O because of 100% conversion for NH_3 at each temperature (Figure 3b) and the fact that all the NH_3 was consumed according to Equation (4). However, the latter catalyst generated ca. 25 ppm N_2O at 450 °C (Figure 4), which is only a half of the concentration of N_2O expected using Equation (4), while the unpromoted one did ca. 110 ppm N_2O at 480 °C, which is over twice as high as the expected N_2O (Figure 4). These points represent that the VWT-only could produce N_2O via Equation (3) and that Fe_2O_3 species added to VWT can depress N_2O emissions in NH_3-SCR reaction. Such a role is probable, with an assumption not only that the promoted VWT could have more abundant NH_3 species strongly adsorbed on the

surface but also that the NH_3 could readily reduce N_2O produced [24]. This surface reaction can be successfully described as the overall stoichiometry [16,20,21],

$$4N_2O + 4NH_3 + O_2 \rightarrow 6N_2 + 6H_2O, \quad (6)$$

and it is consistent with earlier studies that N_2O has been easily reduced by NH_3 over Fe-zeolites [20,21,40]. Furthermore, this pathway to decrease N_2O production was very similar to that reported in our previous work for a commercial V_2O_5-WO_3/TiO_2 catalyst coated by Fe-ZSM-5 [16], indicating that Fe_2O_3 is promised as a much cheaper, simpler promoter for significant reduction in N_2O emissions in NH_3-SCR reaction at high temperatures. On the other hand, 2.73% Fe_2O_3/c-VWT and c-VWT both showed much lower N_2O concentrations than maximum values that can be reached by only a single pathway of Equation (4) at similar a NO conversion to each other (Figures 3a and 4). Besides this, all the catalysts above 350 °C gave lesser N_2O production than those over the unpromoted and promoted VWT (Figure 4). It suggests that the c-VWT-based catalysts may possess much greater ability to catalyze Equation (6). Surface chemistry regarding this reaction occurring on the Fe_2O_3-promoted VWT and c-VWT catalysts will be evident in NH_3 TPD (temperature-programmed desorption) measurements below.

2.4. Role of Fe_2O_3 Species for the Suppression of N_2O Formation

In the TPD of NH_3 adsorbed on VWT, 2.73% Fe_2O_3/VWT, c-VWT, and 2.73% Fe_2O_3/c-VWT, mass spectra for the releasing NH_3 and gaseous products such as H_2O, N_2O, NO, and N_2 are provided in Figures 5 and 6. Predominant desorption of the adsorbed NH_3 occurred at temperatures ranging from 225 to 275 °C with bumps at 370–425 °C and high-temperature peaks at 650–690 °C, depending on the catalyst, as shown in spectra S1 to S4 in Figure 5a. Both a downward-shift of a maximum desorption temperature by 20–35 °C and an appreciable increase of the 650–690 °C NH_3 occurred on the Fe_2O_3-promoted samples (Figure 5a(S2,S4)). This implies that although the Fe_2O_3 species weakened the acid strength of sites for NH_3 desorbing at relatively low temperature region, they could significantly increase very stable NH_3 species. This agrees well with the discussion above. Figure 5b shown for H_2O generation is indicative of the oxidation of the adsorbed NH_3 to the N-containing products. The H_2O gave peaks with maxima around 250–260, 450–470, and 645–660 °C, depending on the sample (Figure 5b(S1–S4)). A relatively much higher H_2O production at the 645–660 °C region was detected for c-VWT and 2.73% Fe_2O_3/c-VWT (Figure 5b(S3,S4)), proposing that these catalysts can, to a much greater extent, oxidize the adsorbed NH_3 species into the N-containing gases, as shown below.

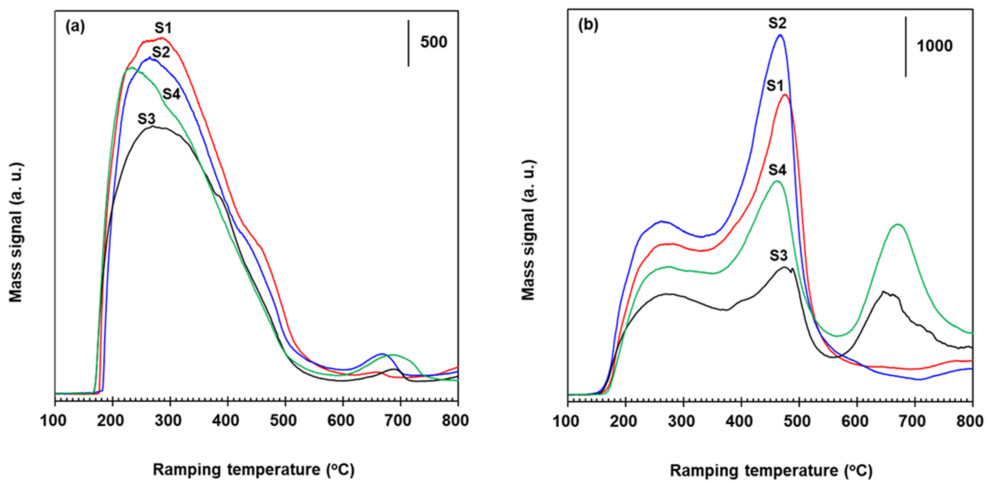

Figure 5. Mass spectra for NH_3 desorbed and H_2O produced during NH_3 TPD runs with unpromoted and Fe_2O_3-promoted catalysts: (**a**) NH_3 and (**b**) H_2O. In (**a**) and (**b**), S1: VWT; S2: 2.73% Fe_2O_3/VWT; S3: c-VWT; S4: 2.73% Fe_2O_3/c-VWT.

Mass spectra for N_2O, NO, and N_2 in the NH_3 TPD runs with the bare and Fe_2O_3-promoted catalysts are provided in Figure 6. All these catalysts gave major NO peaks having a maximum at 240–280 °C with shoulders at 375–415 and 480–495 °C, and relatively small peaks at temperatures >570 °C (Figure 6a). The last peaks are indirect evidence of NH_3-related species strongly adsorbed on the catalyst surface. It is clear that NH_3 adsorbed on the catalysts reacts with labile surface oxygen atoms existing in VO_x, FeO_x, and WO_x to create gaseous NO [41,42]. The most appropriate overall stoichiometry of this surface reaction can be described using Equation (5). Of course, the extent of the NO formation is small when the indicated size of the vertical solid bar in Figures 5 and 6 was compared each other.

Figure 6b shows N_2O production whose peaks at 270–285, 445–490, and 650–680 °C appear. Their intensity greatly depended on the catalyst, as seen in spectra S1–S4. c-VWT had an additional peak at 780 °C and showed a N_2O production profile similar to that reported for another commercial 1.68% V_2O_5-7.6% WO_3/TiO_2 catalyst [16]. The 780 °C N_2O peak disappeared after promotion with 2.73% Fe_2O_3 (Figure 6b(S4)). All these N_2O peaks might come from NH_4^+-like species on Bronsted acid sites such as W^{5+}-OH and WO_3-induced V^{4+}-OH, and from NH_x moieties (x = 1–3) adsorbed on Lewis acid sites, VO_x, WO_x, and FeO_x [43–45]. Both α-Fe_2O_3 and γ-Fe_2O_3 have no Bronsted acidity [46,47]. An intensity of the 650–680 °C N_2O peak in VWT and 2.73% Fe_2O_3/VWT (S1 and S2) was very weak compared to that in the other samples (S3 and S4), which is in excellent agreement with the H_2O production levels (Figure 5b). All the unpromoted catalysts (spectra S1 and S3 in Figure 6b) gave N_2O peaks at 490 °C. This temperature was shifted to 445 °C over Fe_2O_3-promoted samples (S2 and S4), implying that the Fe_2O_3 allows a decrease in the activation energy for the oxidation of adsorbed NH_3 to N_2O. The promoted catalysts showed lesser N_2O emissions in NH_3-SCR reaction (Figure 4). It is well-known that direct oxidation of NH_3 to N_2 and N_2O, not via adsorbed NH_x species (x = 1 or 2), is improbable and NH species on V^{5+}=O sites reacts with gas-phase NO to form N_2O and V^{4+}-OH [11,39,48]. This represents that gaseous NO is essential for such N_2O production, suggesting an involvement of NO molecules shown in Figure 6a because of no feed of NO upon NH_3 TPD experiments.

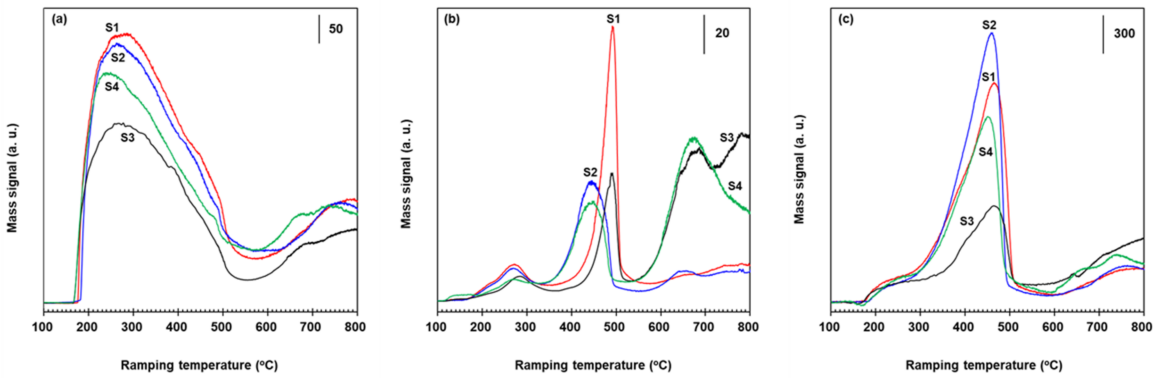

Figure 6. Mass spectra for the production of (**a**) NO, (**b**) N_2O, and (**c**) N_2 in NH_3 TPD runs with unpromoted and promoted VWT-based catalysts. In (**a**–**c**), S1: VWT; S2: 2.73% Fe_2O_3/VWT; S3: c-VWT; S4: 2.73% Fe_2O_3/c-VWT.

Mass spectra for N_2 evolved in NH_3 TPD runs with the unpromoted and promoted catalysts are shown in Figure 6c. Each catalyst had a predominant peak at 450–465 °C with a shoulder at 280–350 °C and a broad peak at temperatures >600 °C, depending on the sample, as seen in profiles S1–S4. As for NO and N_2O in Figure 6a,b, all those N_2 peaks would be associated with ammonium ions and NH_x on Bronsted and Lewis acid centers [43–45]. The NH_x species are oxidized to N_2 via NO-assistant route, as discussed [11,39,48]. The presence of Fe_2O_3 in VWT and c-VWT caused not only a shift of the major N_2 peak to lower temperatures, by 5–15 °C, but also a significant increase in their intensity,

and such changes were greater for the commercial-based catalysts (Figure 6c(S3,S4)). These are in good accordance with the observed trend in the water production of H_2O as an indicator of N-associated side reactions (Figure 5b). It is thought that the promotion by amorphous iron oxide particles can decrease the activation energy for the oxidation of the adsorbed NH_3 species into N_2 and significantly enhance this reaction.

Based on the results in NH_3 TPD experiments with the unpromoted and 2.73% Fe_2O_3-promoted catalysts, and the previous discussion, the iron oxide promotion could significantly increase surface NH_3 species, producing the 650–690 °C peak (Figure 5a), and this ammonia species can be oxidized to NO, N_2O, and N_2 at high temperatures >550 °C (Figure 6). The presence of the Fe_2O_3 is, to some extent, responsible for the loss in deNO_x activity at temperatures >400 °C due to the NO formation (Figure 3a). The NO formed via Equation (5) and/or NO in the feed stream may act as an intermediate for the N_2O and N_2 production [11,39,48]. Thus, Equation (3) rather than Equation (4) may be a main route for the formation of N_2O in NH_3-SCR reaction at temperatures >350 °C, and according to Equation (6), the N_2O can be easily reduced by the strongly-adsorbed NH_3 species on Fe_2O_3 and/or its related surface complex interacting with surface V_2O_5 species, thereby producing less N_2O in NH_3-SCR reaction with the promoted catalysts (Figure 4). This proposal is similar to that reported for great reduction in N_2O emissions over Fe-zeolites alone and Fe-ZSM-5-coated V_2O_5-WO_3/TiO_2 catalysts [16,20,21,23,40]. Consequently, Fe_2O_3 species existing in V_2O_5/TiO_2-based catalysts play a significant role for the suppression of N_2O formation in NH_3-SCR reaction at high temperature side, and this approach is a much simpler and more cost-effective compared to Fe-zeolite promotion techniques.

2.5. Surface Structure of Fe_2O_3, V_2O_5, and WO_3 Species

Figure 7 shows Raman spectra for reference materials and WT whose original signals have been reduced by 1/10–1/1000 for an easier comparison, but all bands have been kept unchanged even after such a data processing. α-phase V_2O_5 polycrystallites yielded a sharp peak at 990 cm^{-1} with subsequent signals near 400, 470, 515, and 700 cm^{-1}, as seen in Figure 7a. Crystalline WO_3 had characteristic sharp bands around 800 and 715 cm^{-1} (Figure 7b), and no Raman signals at frequencies >800 cm^{-1} even in a magnified spectrum existed as indicated by the dashed line. The measured spectra for the V_2O_5 and monoclinic γ-WO_3 ($P2_1/n$) are in agreement with earlier studies [49,50]. Bands due to highly-dispersed amorphous WO_x in a sample of WT that has been employed for preparing VWT and 2.73% Fe_2O_3/VWT catalysts can be differentiated by comparing with those existing in a bare anatase TiO_2 (Figure 7c,d). This support had Raman signals at 397, 515, and 638 cm^{-1} (Figure 7c) with a predominant band at 145 cm^{-1} and a weak one at 197 cm^{-1} (not shown here). The 397, 515 and 145, and 197 and 638 cm^{-1} bands correspond to the respective B_{1g}, A_{1g} + B_{1g} and E_g phonon vibrations of anatase-type TiO_2 [49,51–53]. A weak signal at 793 cm^{-1} (see the magnified spectrum in Figure 7c) is due to the first overtone of the 395 cm^{-1} [49,52,53]. Besides these peaks, bands at 882 and 980 cm^{-1} existed in the WT sample, as provided in the magnified spectrum in Figure 7d. The 980 cm^{-1} peak is assigned to two-dimensional polytungstate species with distorted octahedrally-coordinated environments that have been reported for calcined WO_3/TiO_2 samples not exceeding a monolayer coverage [53,54]. The 882 cm^{-1} is associated with asymmetric W-O-W vibrations in polymeric surface WO_x species [53]. It is represented that the WT sample has two different surface WO_x species. The absence of the 800 and 715 cm^{-1} bands reveals no crystalline WO_3 particles, indicating a very good dispersion of the tungsten oxide on the titania.

Raman spectra for VWT, 2.73% Fe_2O_3/VWT, c-VWT, and 2.73% Fe_2O_3/c-VWT are provided in Figure 8. All the catalysts had bands near 394, 515, 636, and 790 cm^{-1}, that are due to the TiO_2 support (Figure 7c), and they all also produced peaks at 880 and 981 cm^{-1} (Figure 7a–d). Any of the catalysts indicated no band near 1020–1030 cm^{-1} regarding isolated surface VO_x species [35,55]. The 981 and 880 cm^{-1} peaks had appeared even in the WT-only sample (Figure 7d). Regardless, these two bands may not be originated from the W=O and W-O-W structures in the surface tungsten oxide species. Symmetric V=O and W=O stretching vibrations occur at 950–990 cm^{-1}, making it

difficult to clearly distinguish between both species, but the V=O species have an interaction cross section that is almost four times greater than that of the W=O groups [53,55–57]; thus, a Raman signal by the V=O structures in surface vanadium oxide species would give much stronger intensity at the frequency region. Furthermore, it has been reported not only for no appreciable mutual effect on the surface structures of VO_x and WO_x species in V_2O_5-WO_5/TiO_2 systems with low total VO_x and WO_x coverages but also for Raman bands at 940–987 cm^{-1}, due to two-dimensional VO_x species in 1–4.5% V_2O_5/TiO_2 below a monolayer coverage, whose positions are usually higher, by 10–30 cm^{-1}, than that of surface WO_x species in 1–7% WO_3/TiO_2 [55,58]. Consequently, the 880 and 981 cm^{-1} bands correspond to the respective bridging V-O-V and terminal V=O structures in distorted octahedrally coordinated VO_6 species, even in the TiO_2-supported binary and ternary component systems employed here, and indicate the presence of polymerized mono-oxo vanadate species [49,53,55,56,58].

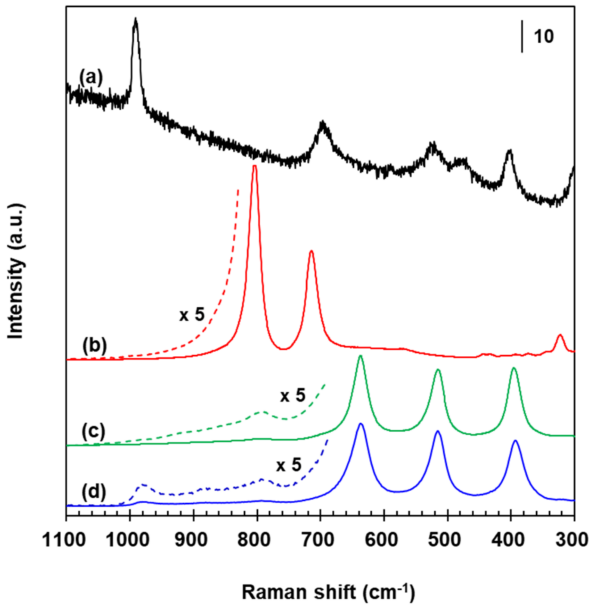

Figure 7. Raman spectra for reference chemicals and a supported WO_3-only sample: (**a**) V_2O_5; (**b**) WO_3; (**c**) TiO_2; (**d**) 10% WO_3/TiO_2 (WT).

All the iron oxides discussed in the XRD measurements, except for magnetite, exhibit Raman bands at 1000–1600 cm^{-1} in which no Raman signals by TiO_2 appear [30,49,51,59]. However, all the 2.73% Fe_2O_3-promoted catalysts gave no bands in the frequency region as well as at 800–1100 cm^{-1} (Figure 8b,d). The latter is because of the absence of Fe=O bonds in the iron oxides. Of course, bands below 800 cm^{-1} by Fe-O in surface iron oxide species could not be visible due to very intense signals of the titania support itself. All the promoted samples also gave no peaks near 1320, and 1375 and 1580 cm^{-1} for crystalline α- and γ-Fe_2O_3, respectively [30]. The intensity of all the characteristic vibration modes of the support was maintained unchanged even after the addition of 2.73% Fe_2O_3 to VWT and c-VWT, proposing that no great interaction of the iron oxide species with the titania surface occurred. There is no indication of the formation of V_2O_5, WO_3, and Fe_2O_3 crystals even in the titania-supported ternary systems, consistent with the previous discussion in the XRD measurements (Figure 1). This indicates that they all consist of submonolayer coverage of the metal oxides species. Table 2 lists the surface density of each metal oxide existing in the unpromoted and promoted catalysts that was estimated using its amount and their S_{BET} value given in Table 1. Calculations of the surface coverage based on monolayer coverage of each metal oxide reported in the literature [60–66] are also provided in Table 2. Both VO_x and FeO_x were below monolayer coverage irrespective of the catalyst, but WO_x in VWT, 2.73% Fe_2O_3/VWT and c-VWT could exceed the monolayer coverage, which is mainly due to a rather wide range of experimentally-determined WO_x monolayer values, such as

4.6–7.0 μmol WO_x/m^2 [60,61,63,65,66]. The upper limit can give us a value near monolayer coverage. The calculated coverages are in reasonable agreement with the Raman measurements. The total surface coverage expressed as MeO_x in Table 2 can be similarly explained, even though it was somewhat high for 2.73% Fe_2O_3/VWT. Finally, c-VWT after Fe_2O_3 promotion indicated a decrease in the surface coverages of each component, as well as of MeO_x, consistent with the redispersion of V_2O_5 in the promoted catalyst (Figure 1d).

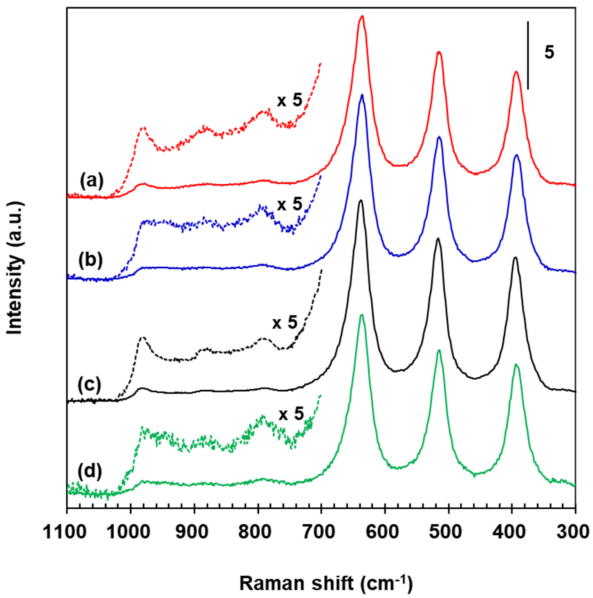

Figure 8. Raman spectra for unpromoted and promoted V_2O_5/TiO_2-based catalysts: (**a**) VWT; (**b**) 2.73% Fe_2O_3/VWT; (**c**) c-VWT; (**d**) 2.73% Fe_2O_3/c-VWT.

The noticeable difference between the unpromoted samples and the promoted ones is a new shoulder around 945 cm^{-1}, broadening of the 981 cm^{-1} band, and appreciable weakening of the phonon intensity of the 880 cm^{-1} signal associated with polymeric surface VO_x species (see the magnified spectra in Figure 8b,d). These strongly suggest an alteration of the molecular structure of surface vanadia and/or tungsta species when 2.73% Fe_2O_3 was introduced to VWT and c-VWT. However, it does not seem that there was a great structural interaction between the surface VO_x species and the FeO_x species, since the position of the 880 and 981 cm^{-1} bands is the same even after the promotion [61]. The terminal V=O band broadening is because of small interactions between the surface metal oxides, perhaps VO_x and FeO_x [55,60,63]. This was indicated by the disappearance of the XRD peak due to V_2O_5 in 2.73% Fe_2O_3/c-VWT (see Figure 1c,d), although such a change was not visible for VWT and 2.73% Fe_2O_3/VWT. The interaction can increase the extent of the disorder of the catalyst surface, and this becomes more energetically heterogeneous, suggesting that an enhancement to the main NH_3-SCR routes and/or the side reactions over the promoted catalysts is probable. The new signal at 945 cm^{-1} may be associated with rearrangement of the polymeric surface VO_x species, because it appeared with the weakening of the 880 cm^{-1} band. All samples of V_2O_5/TiO_2 and V_2O_5-WO_3/TiO_2 with low total surface coverage exhibited signals near 945 cm^{-1} in their Raman spectra collected at ambient conditions, and these were assigned to surface metavanadate species [55]. On the other hand, not only a significant electronic interaction between Fe^{3+} species and V^{5+} ones in titania-supported iron vanadates that are highly active for NH_3-SCR reaction could be evident from the Fe and V K-edge X-ray absorption, but a reduced oxidation capability of the vanadium oxide in the V-O-Fe species was alsoproposed to give a better N_2 selectivity at high temperatures >300 °C [67]. Combining our Raman results with the earlier reports suggests that the tetrahedrally coordinated

polymeric vanadates adjacent to Fe_2O_3 species play a role in the reduction of N_2O formed in NH_3-SCR reaction at high temperatures by strongly-adsorbed NH_3 residues.

Table 2. Surface density and surface coverages of the active ingredients in V_2O_5/TiO_2-based catalysts.

Catalyst	Surface Density (μmol/m^2)				Surface Coverage			
	VO_x	WO_x	FeO_x	MeO_x [a]	VO_x [b]	WO_x [c]	FeO_x [d]	MeO_x [e]
WT	-	4.74	-	4.74	-	0.86 ± 0.17	-	0.86 ± 0.17
VWT	2.63	6.44	-	9.07	0.22 ± 0.02	1.16 ± 0.24	-	1.38 ± 0.26
2.73% Fe_2O_3/VWT	2.93	7.19	5.69	15.81	0.24 ± 0.03	1.30 ± 0.26	0.87	1.54 ± 0.29
c-VWT	2.26	5.80	-	8.06	0.19 ± 0.02	1.05 ± 0.21	-	1.24 ± 0.23
2.73% Fe_2O_3/c-VWT	1.78	4.57	3.84	10.19	0.15 ± 0.01	0.82 ± 0.17	0.59	0.97 ± 0.18

Note. "-": not applicable or measured. [a] Sum of the surface density values for VO_x, WO_x, and FeO_x. [b] Based on monolayer coverage of 10.9–13.1 μmol VO_x/m^2 [60–64]. [c] Based on monolayer coverage of 4.6–7.0 μmol WO_x/m^2 [60,61,63,65,66]. [d] Based on monolayer coverage of ca. 6.5 μmol FeO_x/m^2 [61,63]. [e] Sum of the surface coverages of VO_x, WO_x, and FeO_x.

3. Experimental

3.1. Preparation of Catalyst Samples

A commercial powder-type 10% WO_3/TiO_2 (Tronox Ltd., formerly Kerr-McGee Corp., Stamford, CT, USA), hereafter designated to "WT", was employed to prepare a V_2O_5-WO_3/TiO_2 catalyst. An appropriate amount of the WT (ca. 10 g) was calcined at 500 °C for 4 h in flowing 21% O_2/79% N_2 (Praxair, 99.999%, Changwon, Korea) at a total flow rate of 300 cm^3/min. A 1.6% V_2O_5/WT catalyst was prepared by impregnating the calcined WT with an aqueous NH_4VO_3 (Aldrich, 99.99%, Saint Louis, MO, USA) solution with the corresponding vanadium content, which had been obtained by dissolving it in an aqueous solution of oxalic acid (Aldrich, ≥99%) with a pH near 2.5 dissolved in distilled, deionized water (DDI), referred to as "VWT". A part of this sample was used for the preparation of approximately 5 g 2.73% Fe_2O_3/VWT that was made by impregnating the VWT with a aqueous solution of $Fe(NO_3)_3 \cdot 9H_2O$ (Aldrich, ≥99.95%) dissolved in DDI water. A commercial extruded V_2O_5-WO_3/TiO_2 honeycomb was supplied from a domestic coal-fired power plant and crushed, finely ground, and calcined as for the WT, denoted to "c-VWT" to differentiate it from the VWT. A 2.73% Fe_2O_3/c-VWT catalyst was prepared using the calcined c-VWT in a fashion similar to that described for the VWT-supported iron oxide. All the catalysts used were dried at 110 °C overnight in an oven and then calcined as for the WT prior to using them for NH_3-SCR reaction and characterization. The N_2 and O_2 used were further purified by passing them through moisture trap and Oxytraps (Alltech Assoc., Deerfield, IL, USA). The amounts of V_2O_5 and WO_3 existing in the c-VWT were determined using ICP (inductively-coupled plasma) measurements.

3.2. NH_3-SCR deNO_x Reaction and Determination of N_2O Formation

Details of the modified Model MARS 0.75 L/8.0 V White gas cell (Zemini Scientific Instr., Buena Park, CA, USA) combined with a Thermo Electron Nicolet 7600 FT-IR spectrophotometer (Thermo Fisher Scientific, Waltham, MA, USA) used in the present study to measure conversions of NO and NH_3 and the extent of N_2O production in NH_3-SCR reaction have been described earlier [6,68]. A continuous purge of this system was allowed by flowing a compressed air at a rate of 15 L/min that had passed through a train of large volume silica traps to remove H_2O in the air. The NH_3-SCR reaction with catalyst samples was conducted in a continuous flow type I-shaped 3/8″ OD quartz reactor placed in a three-independent temperature adjustable electric furnace (Lindberg/Blue M Model HTF55347C, Thermo Electron Corp., Asheville, NC, USA) coupled with a Lindberg/Blue M Model CC584343PC PID controller [6,16,27,68]. All gas feed lines were maintained at a temperature near 180 °C to prevent the homogeneous reaction between NO and O_2, and the condensation of H_2O produced in the reaction.

A flowing mixture of 21% O_2/79% N_2 at a total rate of 1000 cm^3/min was flowed through the reactor with typically 0.5 g catalyst sample to calcine it at 500 °C for 1 h, and then the temperature and oxygen concentration were changed to 200 °C and 5%, respectively. After this, the downstream was switched to the upstream, at which point the gas cell was fully purged prior to recording a background interferogram that was used for Fourier-transforming sample interferograms. Then NO and NH_3 were added to the gas flow so as to be 500 ppm, respectively. An interferogram before reaction was collected at their steady-state concentration. Following this, the gas mixture was flowed over the catalyst bed at chosen temperatures, corresponding to a gas hourly space velocity of 76,200 h^{-1}, and a sample interferogram was obtained after ca. 30 min. All interferograms were collected with a resolution of 0.5 cm^{-1} and a scan number of 100. The NO (Omega grade, 99.99%, Scott Specialty Gases, South Plainfield, NJ, USA) and NH_3 (Scott Specialty Gases, Electronic grade, 99.999%) were used without any purification, while the N_2 was flowed through an Alltech moisture trap. All gas flows were accurately controlled by using a Model 5850E mass flow controller (Brooks Instr., Hatfield, PA, USA) and a Model F-200CV one (Bronkhorst High-Tech, Ruurlo, The Netherland). Details of the standard procedures to collect the gas-phase spectra have been provided elsewhere [6,68].

3.3. Characterization of Catalyst Samples

A Model D/MAX2500 PC diffractometer (Rigaku, Tokyo, Japan) with a Cu Kα (λ = 1.5405 Å) radiation source was employed for XRD measurements in which an X-ray tube voltage and current were 40 kV and 20 mA, respectively. Each calcined sample charged in a thin quartz holder was scanned from a 2θ value of 10 to 80° at a scanning rate of 0.1°/min to allow an accurate resolution.

A Model 3 Flex Version 3.01 system (Micromeritics Instr., Norcross, GA, USA) was used to determine textural properties of the catalysts, such as S_{BET}, d_m, and V_t. A cell containing ca. 60 mg of each sample was directly connected to the system, evacuated at 300 °C overnight (under a high dynamic vacuum below 10^{-7} Torr (1 Torr = 133.3 Pa)) and allowed for a further evacuation at room temperature. Following this, N_2 was introduced into the sample cell at a liquid nitrogen temperature (−196 °C).

Temperature-programmed desorption (TPD) studies were conducted using a Model HPR-20 QIC quadrupole mass (Hiden Analytical, Warrington, UK) spectrometer system described in detail elsewhere [16,69,70]. For this, an adsorption cell with 160 mg of each sample was coupled with a gas handling system to calcine at 500 °C for 1 h in a flowing mixture of 21% O_2/79% He (Praxair, 99.9999%) at a total flow rate of 100 cm^3/min. Then, 2% NH_3 in flowing He at the same flow rate was admitted to the cell at 100 °C for 1 h prior to fully purging it using the pure He flow. After the NH_3 approached a background level, it was heated to 800 °C at 10 °C/min in a He flow at a total rate of 20 cm^3/min. During this process, N-containing products, i.e., N_2O, NO, and N_2, were monitored at each corresponding m/z, but NH_3 desorbed was monitored at m/z = 16, because H_2O formed upon the surface reaction, producing the nitrogenous products that could be fragmentized to OH [16,69]. All the gases were controlled using a Model 5850E mass flow controller (Brooks Instr., Hatfield, PA, USA). The He used has been further purified in a similar fashion as described above.

Ex situ Raman spectra for fresh catalysts calcined in a fashion similar to that described for the activity measurements were recorded in the range of 50–3400 cm^{-1} with a 2 cm^{-1} spectral resolution. V_2O_5 (Aldrich, 99.99%), WO_3 (99.995%), TiO_2 (DT51D, Millennium Inorganic Chemicals, Henderson, Australia), and the WT were used as a reference material. The measurements were conducted using a Thermo Scientific DXR 2xi Raman spectrometer (Thermo Fisher Scientific, Waltham, MA, USA) equipped with a liquid N_2-cooled EM-CCD detector around −120 °C. A 532-nm diode laser was employed to excite the samples. A power of the laser at a surface of each sample was applied to be ca. 2 mW in order to minimize laser heating effects. Exposure of each sample to the laser beam was approximately 0.01–0.03 s with 500 to 800 averaged signal accumulations, depending on the sample. All spectra were collected with a powder under ambient conditions.

4. Conclusions

Fe_2O_3-promoted V_2O_5/TiO_2-based catalysts show no great changes in the textural features, and no XRD peaks due to crystalline Fe_2O_3 phases are indicated. Significant depression of N_2O emissions in NH_3-SCR reaction over V_2O_5-WO_3/TiO_2 catalysts at high temperatures could be successfully established by their promotion using Fe_2O_3 particles. This approach results in a decrease in NO conversion at high temperatures, which is mainly because of the oxidation of NH_3 to NO. NH_3 TPD measurements suggest that the Fe_2O_3 existing in VWT and c-VWT can significantly increase strongly-adsorbed NH_3 and NH_x moieties, and these species participate in the reduction of N_2O formed at high temperatures. Raman spectra for the promoted catalysts propose the presence of Fe_2O_3-induced, tetrahedrally coordinated polyvanadates and/or surface V-O-Fe species that are probably responsible for the N_2O reduction. The reaction between NO and NH_3 may predominantly take place to form N_2O that can be readily reduced by the strongly adsorbed NH_3 over the Fe_2O_3-promoted catalysts.

Acknowledgments: A partial grant-in-aid for this study was provided by Basic Science Research Program through the National Research Foundation of Korea (NRF) via Grant # 2017080772.

Author Contributions: The key approach to this study was designed by Moon Hyeon Kim who also determined a significance of all data and wrote this manuscript. Ki Hyuck Yang performed the experiments regarding activity measurements and instrumental characterization. He also prepared a draft version of all Figures included here. The co-authors have made an approval of the final version of this manuscript.

Conflicts of Interest: The authors declare no conflict of interest.

References

1. Marberger, A.; Elsener, M.; Ferri, D.; Krocher, O. VO_x surface coverage optimization of V_2O_5/WO_3-TiO_2 SCR catalysts by variation of the V loading and by aging. *Catalysts* **2015**, *5*, 1704–1720. [CrossRef]
2. He, Y.; Ford, M.E.; Zhu, M.; Liu, Q.; Tumuluri, U.; Wu, Z.; Wachs, I.E. Influence of catalyst synthesis method on selective catalytic reduction (SCR) of NO by NH_3 with V_2O_5-WO_3/TiO_2 catalysts. *Appl. Catal. B* **2016**, *193*, 141–150. [CrossRef]
3. Madia, G.; Elsener, M.; Koebel, M.; Raimondi, F.; Wokaun, A. Thermal stability of vanadia-tungsta-titania catalysts in the SCR process. *Appl. Catal. B* **2002**, *39*, 181–190. [CrossRef]
4. Forzatti, P. Present status and perspectives in de-NO_x SCR catalysis. *Appl. Catal. A* **2001**, *222*, 221–236. [CrossRef]
5. Nova, I.; dall'Acqua, L.; Lietti, L.; Giamello, E.; Forzatti, P. Study of thermal deactivation of a de-NO_x commercial catalyst. *Appl. Catal. B* **2001**, *35*, 31–42. [CrossRef]
6. Kim, M.H.; Ham, S.W. Determination of N_2O emissions levels in the selective reduction of NO_x by NH_3 over an on-site-used commercial V_2O_5-WO_3/TiO_2 catalyst using a modified gas cell. *Top. Catal.* **2010**, *53*, 597–607. [CrossRef]
7. Kompio, P.G.W.A.; Bruckner, A.; Hipler, F.; Auer, G.; Loffler, E.; Grunert, W. A new view on the relations between tungsten and vanadium in V_2O_5-WO_3/TiO_2 catalysts for the selective reduction of NO with NH_3. *J. Catal.* **2012**, *286*, 237–247. [CrossRef]
8. Lietti, L.; Nova, I.; Ramis, G.; Dall'Acqua, L.; Busca, G.; Giamello, E.; Forzatti, P.; Bregani, F. Characterization and reactivity of V_2O_5–MoO_3/TiO_2 de-NO_x SCR catalysts. *J. Catal.* **1999**, *187*, 419–435. [CrossRef]
9. Nova, I.; Ciardelli, C.; Tronconi, E.; Chatterjee, D.; Weibel, M. Unifying redox kinetics for standard and fast NH_3-SCR over a V_2O_5-WO_3/TiO_2 catalyst. *AIChE J.* **2009**, *55*, 1514–1529. [CrossRef]
10. Nova, I.; Ciardelli, C.; Tronconi, E.; Chatterjee, D.; Bandl-Konrad, B. NH_3-NO/NO_2 chemistry over V-based catalysts and its role in the mechanism of the fast SCR reaction. *Catal. Today* **2006**, *114*, 3–12. [CrossRef]
11. Xiong, S.; Xiao, X.; Liao, Y.; Dang, H.; Shan, W.; Yang, S. Global kinetic study of NO reduction by NH_3 over V_2O_5–WO_3/TiO_2: Relationship between the SCR performance and the key factors. *Ind. Eng. Chem. Res.* **2015**, *54*, 11011–11023. [CrossRef]
12. Koebel, M.; Madia, G.; Elsener, M. Selective catalytic reduction of NO and NO_2 at low temperatures. *Catal. Today* **2002**, *73*, 239–247. [CrossRef]

13. Madia, G.; Koebel, M.; Elsener, M.; Wokaun, A. Side reactions in the selective catalytic reduction of NO_x with various NO_2 fractions. *Ind. Eng. Chem. Res.* **2002**, *41*, 4008–4015. [CrossRef]
14. Djerad, S.; Crocoll, M.; Kureti, S.; Tifouti, L.; Weisweiler, W. Effect of oxygen concentration on the NO_x reduction with ammonia over V_2O_5–WO_3/TiO_2 catalyst. *Catal. Today* **2006**, *113*, 208–214. [CrossRef]
15. Kim, M.H.; Lee, H.S. Effect of Fe-zeolite on formation of N_2O in selective reduction of NO by NH_3 over V_2O_5-WO_3/TiO_2 catalyst. *Res. Chem. Intermed.* **2016**, *42*, 171–184. [CrossRef]
16. Kim, M.H.; Park, S.W. Selective reduction of NO by NH_3 over Fe-zeolite-promoted V_2O_5-WO_3/TiO_2-based catalysts: Great suppression of N_2O formation and origin of NO removal activity loss. *Catal. Commun.* **2016**, *86*, 82–85. [CrossRef]
17. Krocher, O.; Elsener, M. Combination of V_2O_5/WO_3-TiO_2, Fe-ZSM5, and Cu-ZSM5 catalysts for the selective catalytic reduction of nitric oxide with ammonia. *Ind. Eng. Chem. Res.* **2008**, *47*, 8588–8593. [CrossRef]
18. Yang, S.; Wang, C.; Ma, L.; Peng, Y.; Qu, Z.; Yan, N.; Chen, J.; Chang, H.; Li, J. Substitution of WO_3 in V_2O_5/WO_3-TiO_2 by Fe_2O_3 for selective catalytic reduction of NO with NH_3. *Catal. Sci. Technol.* **2013**, *3*, 161–168. [CrossRef]
19. Gao, R.; Zhang, D.; Liu, X.; Shi, L.; Maitarad, P.; Li, H.; Zhang, J.; Cao, W. Enhanced catalytic performance of V_2O_5-$WO_3/Fe_2O_3/TiO_2$ microspheres for selective catalytic reduction of NO by NH_3. *Catal. Sci. Technol.* **2013**, *3*, 191–199. [CrossRef]
20. Devadas, M.; Krocher, O.; Elsener, M.; Wokaun, A.; Mitrikas, G.; Soger, N.; Pfeifer, M.; Demel, Y.; Mussmann, L. Characterization and catalytic investigation of Fe-ZSM5 for urea-SCR. *Catal. Today* **2007**, *119*, 137–144. [CrossRef]
21. Qi, G.; Yang, R.T. Ultra-active Fe/ZSM-5 catalyst for selective catalytic reduction of nitric oxide with ammonia. *Appl. Catal. B* **2005**, *60*, 13–22. [CrossRef]
22. Rivallan, M.; Ricchiardi, G.; Bordiga, S.; Zecchina, A. Adsorption and reactivity of nitrogen oxides (NO_2, NO, N_2O) on Fe-zeolites. *J. Catal.* **2009**, *264*, 104–116. [CrossRef]
23. Coq, B.; Mauvezin, M.; Delahay, G.; Butet, J.B.; Kieger, S. The simultaneous catalytic reduction of NO and N_2O by NH_3 using an Fe-zeolite-beta catalyst. *Appl. Catal. B* **2000**, *27*, 193–198. [CrossRef]
24. Mou, X.; Zhang, B.; Li, Y.; Yao, L.; Wei, X.; Su, D.S.; Shen, W. Rod-shaped Fe_2O_3 as an efficient catalyst for the selective reduction of nitrogen oxide by ammonia. *Angew. Chem. Int. Ed.* **2012**, *51*, 2989–2993. [CrossRef] [PubMed]
25. Qu, Z.; Miao, L.; Wang, H.; Fu, Q. Highly dispersed Fe_2O_3 on carbon nanotubes for low-temperature selective catalytic reduction of NO with NH_3. *Chem. Commun.* **2015**, *51*, 956–958. [CrossRef] [PubMed]
26. Liu, F.; Asakura, K.; He, H.; Shan, W.; Shi, X.; Zhang, C. Influence of sulfation on iron titanate catalyst for the selective catalytic reduction of NO_x with NH_3. *Appl. Catal. B* **2011**, *103*, 369–377. [CrossRef]
27. Kim, M.H.; An, T.H. A commercial V_2O_5-WO_3/TiO_2 catalyst used at an NH_3-SCR deNO_x process in an oil-fired power plant: Cause of an increase in deNO_xing and NH_3 oxidation performances at low temperatures. *Res. Chem. Intermed.* **2011**, *37*, 1333–1344. [CrossRef]
28. Chen, Y.; Yang, G.; Zhang, Z.; Yang, X.; Hou, W.; Zhu, J.J. Polyaniline-intercalated layered vanadium oxide nanocomposites—One-pot hydrothermal synthesis and application in lithium battery. *Nanoscale* **2010**, *2*, 2131–2138. [CrossRef] [PubMed]
29. Xu, J.; Yang, H.; Fu, W.; Du, K.; Sui, Y.; Chen, J.; Zeng, Y.; Li, M.; Zou, G. Preparation and magnetic properties of magnetite nanoparticles by sol–gel method. *J. Magn. Magn. Mater.* **2007**, *309*, 307–311. [CrossRef]
30. De Faria, D.L.A.; Silva, S.V.; de Oliveira, M.T. Raman microspectroscopy of some iron oxides and oxyhydroxides. *J. Raman Spectrosc.* **1997**, *28*, 873–878. [CrossRef]
31. Thommes, M.; Smarsly, B.; Groenewolt, M.; Ravikovitch, P.I.; Neimark, A.V. Adsorption hysteresis of nitrogen and argon in pore networks and characterization of novel micro- and mesoporous silicas. *Langmuir* **2006**, *22*, 756–764. [CrossRef] [PubMed]
32. Xia, B.; Li, W.; Zhang, B.; Xie, Y. Low temperature vapor-phase preparation of TiO_2 nanopowder. *J. Mater. Sci.* **1999**, *34*, 3505–3511. [CrossRef]
33. Alemany, L.J.; Berti, F.; Busca, G.; Ramis, G.; Robba, D.; Toledo, G.P.; Trombetta, M. Characterization and composition of commercial V_2O_5-WO_5-TiO_2 SCR catalysts. *Appl. Catal. B* **1996**, *10*, 299–311. [CrossRef]
34. Gutierrez, M.J.F.; Baxter, D.; Hunter, C.; Svoboda, K. Nitrous Oxide (N_2O) emissions from waste and biomass to energy plants. *Waste Manag. Res.* **2005**, *23*, 133–147. [CrossRef] [PubMed]

35. Kompio, P.G.W.A.; Bruckner, A.; Hipler, F.; Manoylova, O.; Auer, G.; Mestl, G.; Grunert, W. V_2O_5-WO_3/TiO_2 catalysts under thermal stress: Responses of structure and catalytic behavior in the selective catalytic reduction of NO by NH_3. *Appl. Catal. B* **2017**, *217*, 365–377. [CrossRef]
36. Wang, C.; Yang, S.; Chang, H.; Peng, Y.; Li, J. Dispersion of tungsten oxide on SCR performance of V_2O_5-WO_3/TiO_2: Acidity, surface species and catalytic activity. *Chem. Eng. J.* **2013**, *225*, 520–527. [CrossRef]
37. Lietti, L.; Nova, I.; Forzatti, P. Selective catalytic reduction (SCR) of NO by NH_3 over TiO_2-supported V_2O_5-WO_3 and V_2O_5-MoO_3 catalysts. *Top. Catal.* **2000**, *11*, 111–122. [CrossRef]
38. Busca, G.; Lietti, L.; Ramis, G.; Berti, F. Chemical and mechanistic aspects of the selective catalytic reduction of NO_x by ammonia over oxide catalysts: A review. *Appl. Catal. B* **1998**, *18*, 1–36. [CrossRef]
39. Long, R.Q.; Yang, R.T. Selective catalytic oxidation of ammonia to nitrogen over Fe_2O_3-TiO_2 prepared with a sol–gel method. *J. Catal.* **2002**, *207*, 158–165. [CrossRef]
40. Zhang, X.; Shen, Q.; He, C.; Ma, C.; Cheng, J.; Hao, Z. N_2O catalytic reduction by NH_3 over Fe-zeolites: Effective removal and active site. *Catal. Commun.* **2012**, *18*, 151–155. [CrossRef]
41. Went, G.T.; Leu, L.J.; Rosin, R.R.; Bell, A.T. The effects of structure on the catalytic activity and selectivity of V_2O_5/TiO_2 for the reduction of NO by NH_3. *J. Catal.* **1992**, *134*, 492–505. [CrossRef]
42. Usberti, N.; Jablonska, M.; Blasi, M.D.; Forzatti, P.; Lietti, L.; Beretta, A. Design of a "high-efficiency" NH_3-SCR reactor for stationary applications. A kinetic study of NH_3 oxidation and NH_3-SCR over V-based catalysts. *Appl. Catal. B* **2015**, *179*, 185–195. [CrossRef]
43. Giraud, F.; Geantet, C.; Guilhaume, N.; Loridant, S.; Gros, S.; Porcheron, L.; Kanniche, M.; Bianchi, D. Experimental microkinetic approach of de-NO_x by NH_3 on V_2O_5/WO_3/TiO_2 catalysts. 3. Impact of superficial WO_z and V_xO_y/WO_z groups on the heats of adsorption of adsorbed NH_3 species. *J. Phys. Chem. C* **2015**, *119*, 15401–15413. [CrossRef]
44. Kantcheva, M.M.; Hadjiivanov, K.I.; Klissurski, D.G. An IR spectroscopy study of the state and localization of vanadium-oxo species adsorbed on TiO_2 (anatase). *J. Catal.* **1992**, *134*, 299–310. [CrossRef]
45. Topsoe, N.Y. Characterization of the nature of surface sites on vanadia-titania catalysts by FTIR. *J. Catal.* **1991**, *128*, 499–511. [CrossRef]
46. Lorenzelli, V.; Busca, G. Infrared studies of the surface of α-Fe_2O_3. *Mater. Chem. Phys.* **1985**, *13*, 261–281. [CrossRef]
47. Ramis, G.; Yi, L.; Busca, G.; Turco, M.; Kotur, E.; Willey, R.J. Adsorption, activation, and oxidation of ammonia over SCR catalysts. *J. Catal.* **1995**, *157*, 523–535. [CrossRef]
48. Jung, S.M.; Grange, P. DRIFTS investigation of V=O behavior and its relations with the reactivity of ammonia oxidation and selective catalytic reduction of NO over V_2O_5 catalyst. *Appl. Catal. B* **2002**, *36*, 325–332. [CrossRef]
49. Went, G.T.; Oyama, S.T.; Bell, A.T. Laser Raman spectroscopy of supported vanadium oxide catalysts. *J. Phys. Chem.* **1990**, *94*, 4240–4246. [CrossRef]
50. Boulova, M.; Lucazeau, G. Crystallite nanosize effect on the structural transitions of WO_3 studied by Raman spectroscopy. *J. Solid State Chem.* **2002**, *167*, 425–434. [CrossRef]
51. Ohsaka, T.; Izumi, F.; Fujiki, Y. Raman spectrum of anatase, TiO_2. *J. Raman Spectrosc.* **1978**, *7*, 321–324. [CrossRef]
52. Frank, O.; Zukalova, M.; Laskova, B.; Kurti, J.; Koltai, J.; Kavan, L. Raman spectra of titanium dioxide (anatase, rutile) with identified oxygen isotopes (16, 17, 18). *Phys. Chem. Chem. Phys.* **2012**, *14*, 14567–14572. [CrossRef] [PubMed]
53. Kim, D.S.; Ostromecki, M.; Wachs, I.E. Surface structures of supported tungsten oxide catalysts under dehydrated conditions. *J. Mol. Catal. A* **1996**, *106*, 93–102. [CrossRef]
54. Engweiler, J.; Harf, J.; Baiker, A. WO_x/TiO_2 catalysts prepared by grafting of tungsten alkoxides: Morphological properties and catalytic behavior in the selective reduction of NO by NH_3. *J. Catal.* **1996**, *159*, 259–269. [CrossRef]
55. Vuurman, M.A.; Wachs, I.E.; Hirt, A.M. Structural determination of supported V_2O_5-WO_3/TiO_2 catalysts by in situ Raman spectroscopy and X-ray photoelectron spectroscopy. *J. Phys. Chem.* **1991**, *95*, 9928–9937. [CrossRef]
56. Reiche, M.A.; Burgi, T.; Baiker, A.; Scholz, A.; Schnyder, B.; Wokaun, A. Vanadia and tungsta grafted on TiO_2: Influence of the grafting sequence on structural and chemical properties. *Appl. Catal. A* **2000**, *198*, 155–169. [CrossRef]

57. Wachs, I.E.; Roberts, C.A. Monitoring surface metal oxide catalytic active sites with Raman spectroscopy. *Chem. Soc. Rev.* **2010**, *39*, 5002–5017. [CrossRef] [PubMed]
58. Amiridis, M.D.; Duevel, R.V.; Wachs, I.E. The effect of metal oxide additives on the activity of V_2O_5/TiO_2 catalysts for the selective catalytic reduction of nitric oxide by ammonia. *Appl. Catal. B* **1999**, *20*, 111–122. [CrossRef]
59. Colomban, P.; Cherifi, S.; Despert, G. Raman identification of corrosion products on automotive galvanized steel sheets. *J. Raman Spectrosc.* **2008**, *39*, 881–886. [CrossRef]
60. Bourikas, K.; Fountzoula, C.; Kordulis, C. Monolayer transition metal supported on titania catalysts for the selective catalytic reduction of NO by NH_3. *App. Catal. B* **2004**, *52*, 145–153. [CrossRef]
61. Dunn, J.P.; Stenger, H.G., Jr.; Wachs, I.E. Oxidation of SO_2 over supported metal oxide catalysts. *J. Catal.* **1999**, *181*, 233–243. [CrossRef]
62. Amiridis, M.; Wachs, I.E.; Deo, G.; Jehng, J.M.; Kim, D.S. Reactivity of V_2O_5 catalysts for the selective catalytic reduction of NO by NH_3: Influence of vanadia loading, H_2O, and SO_2. *J. Catal.* **1996**, *161*, 247–253. [CrossRef]
63. Wachs, I.E. Raman and IR studies of surface metal oxide species on oxide supports: Supported metal oxide catalysts. *Catal. Today* **1996**, *27*, 437–455. [CrossRef]
64. Bond, G.C.; Bruckman, K. Selective oxidation of *o*-xylene by monolayer V_2O_5-TiO_2 catalysts. *Faraday Discuss. Chem. Soc.* **1981**, *72*, 235–246. [CrossRef]
65. Vermaire, D.C.; van Berge, P.C. The preparation of WO_3/TiO_2 and $WO_3/A1_2O_3$ and characterization by temperature-programmed reduction. *J. Catal.* **1989**, *116*, 309–317. [CrossRef]
66. Yu, X.F.; Wu, N.Z.; Huang, H.Z.; Xie, Y.C.; Tang, Y.Q. A study on the monolayer dispersion of tungsten oxide on anatase. *J. Mater. Chem.* **2001**, *11*, 3337–3342. [CrossRef]
67. Liu, F.; He, H.; Lian, Z.; Shan, W.; Xie, L.; Asakura, K.; Yang, W.; Deng, H. Highly dispersed iron vanadate catalyst supported on TiO_2 for the selective catalytic reduction of NO_x with NH_3. *J. Catal.* **2013**, *307*, 340–351. [CrossRef]
68. Kim, D.W.; Kim, M.H.; Ham, S.W. An on-line infrared spectroscopic system with a modified multipath White cell for direct measurements of N_2O from NH_3-SCR reaction. *Korean J. Chem. Eng.* **2010**, *27*, 1730–1737. [CrossRef]
69. Kim, M.H.; Cho, I.H.; Park, J.H.; Choi, S.O.; Lee, I.S. Adsorption of CO_2 and CO on H-zeolites with different framework topologies and chemical compositions and a correlation to probing protonic sites using NH_3 adsorption. *J. Porous Mater.* **2016**, *23*, 291–299. [CrossRef]
70. Kim, M.H.; Cho, I.H.; Choi, S.O.; Lee, I.S. Surface energetic heterogeneity of nanoporous solids for CO_2 and CO adsorption: The key to an adsorption capacity and selectivity at low pressures. *J. Nanosci. Nanotechnol.* **2016**, *16*, 4474–4479. [CrossRef] [PubMed]